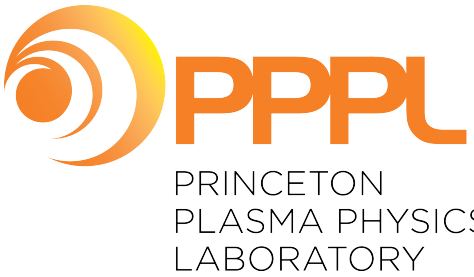

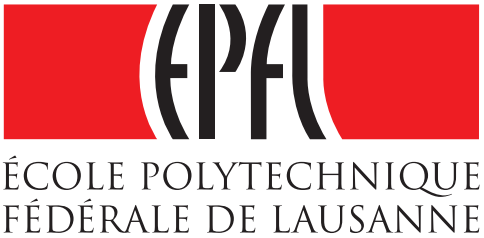

Master Project
Spring 2015

Development of a Synthetic Diagnostics for Beam Emission Spectroscopy

Author:
Loic Hausammann

Supervisor:
Choong-Seock Chang
Michael Churchill
Stephan Brunner

April 24, 2015

Contents

1 Introduction

A synthetic diagnostics consists to simulate the effect of an experimental measurement on the data from a simulation (in this case XGC1). The aim of this kind of measurement is to check if the theoretical model describe well the problem and find the most important effect for the measurement.

The measurement analyzed in this work is the Beam Emission Spectroscopy (BES) that consists to analyze the Balmer-alpha light emission of the excited atoms in a neutral beam. It consists of a Neutral Beam Injector (NBI) and an optical setup, the neutral beam collide with the plasma and, after, emits some photons that will be collected by the optical setup. This diagnostics measures the long wavelength density turbulence in a tokamak, along the radial and poloidal directions ($k_\perp \rho_i \leq 1$[1] where $k_\perp$ is the wave number perpendicular to the magnetic field, and ρ_i is the ion gyro radius). The diagnostics can be applied on the edge and the core.

The aim of the code developed for this report is to be easily adapted for any kind of tokamak (specially the DIII-D and the NSTX). The beam is described with the equilibrium data (therefore does not depend on time) and the emission with the fluctuations.

[1] For DIII-D

2 Beam

The beam is the key element of the BES diagnostics, it is the way that the plasma is perturbed in order to obtain some informations. Usually the BES diagnostics use a diagnostic neutral beam injector and not the heating one due to the energies that are used in the heating, therefore their impact on the plasma are negligible. The aim is to compute the emission due to the beam and, for doing this, the beam density has to be computed.

2.1 Beam attenuation

In order to decrease the computation time, the beam was assumed to be only dependent on the equilibrium data and not the fluctuations. Therefore, it has to be computed only once at the begining and does not depends on the time. The density of the beam (n_b) is modelized with the help of the stopping coefficient (S_{cr})[6]:

$$n_b(P) = n_{b,0} \exp\left(- \int_0^P n_e(z) S_{\text{cr}}\left(E, n_e(z), T_i(z)\right) \sqrt{\frac{m}{2E}} \mathrm{d}z \right) \tag{1}$$

where $n_{b,0}$ is the initial density of the beam, E is the energy of a particle of the beam, n_e is the electron density of the plasma, and m is the mass of a particle in the beam.

The integration is done along the path of a particle, therefore by a straight line parallel to the beam and passing by the point P. For reducing the computation time, the beam is assumed to have always a gaussian profile, thus only a 1D simulation is needed. The code create a mesh bewteen the source of the beam and the farest point used for the optical system. The beam density is computed on this mesh by doing a Gauss-Legendre quadrature formula between theses points. A cubic interpolation is made between the mesh.

The computation of the stopping coefficient is taken in the ADAS database using the ADF21 repository.

2.2 Beam emission

The emissivity is computed with the help of the ADAS database (ADF22) and is given by[3]:

$$\varepsilon(P) = \langle \sigma v \rangle_{\text{ex}} n_e(P) n_b(P), \tag{2}$$

where $\langle \sigma v \rangle_{\text{ex}}$ is the effective beam emission coefficient given by the ADAS database.

2.3 Lifetime effect

The emission of photons is not an instantaneous process, the de-excitation is a process following a decay law ($n(t) = ne^{-t/\tau}$ where n is the density of excited particles) and has a characteristic time given by τ. The characteristic time is the inverse of the Einstein coefficient and depends on the plasma.

In order to compute the emission, the total excited population (n_{ex}) has to be computed. The only value of interest is the new excited particles and assuming a population that is more or less constant over the time scale of the lifetime, it is equivalent to the particles de-excited ($n_{\text{new,ex}} \approx \varepsilon \mathrm{d}t$). The velocity of the fluctuations is assumed to be

negligible in comparison to the beam one and the contribution of the faraway particles is neglected, therefore the total density of population is given by:

$$\begin{aligned} n_{\text{ex}} =& \int_0^{\tau d} \varepsilon(P - tv_b) e^{-t/\tau} \mathrm{d}t \\ =& \frac{1}{\|v_b\|} \int_0^{\tau v_b d} \varepsilon(P - \delta \hat{v}_b) \exp\left(-\frac{\delta}{v_b \tau}\right) \mathrm{d}\delta \end{aligned}$$

where v_b is the beam velocity, $\hat{v}_b = \frac{v_b}{\|v_b\|}$, and d is the cut-off for the faraway particles[2].

Thus the emissivity at the point P is given by:

$$\varepsilon_l(P) = \frac{n_{\text{ex}}(P)}{\tau} \tag{3}$$

The lifetime depends on the collisions and can be computed with the help of the following realation between the excitation and deexcitation rates[5]:

$$\langle \sigma_{ij} v \rangle_{\text{de}} = \frac{g_j}{g_i} \exp\left(\frac{E_{ij}}{T_e}\right) \langle \sigma_{ji} v \rangle_{\text{ex}} \tag{4}$$

where $g_j = 2n_j^2$ (n_j is the principal quantum number), and E_{ij} is the energy difference between the two states. In the case of the Balmer-alpha emission, the value of the index are $(i, j) = (3, 2)$.

From the collision rate, the lifetime can be computed: $\tau = \left(n_e \langle \sigma v \rangle\right)^{-1}$

[2]Usually $d = 4$

Index	Points	Weights
0	$(0,0)$	$\frac{1}{9}$
$1-10$	$\left(hA_{-}\cos\left(\frac{2\pi k}{10}\right), hA_{-}\sin\left(\frac{2\pi k}{10}\right)\right)$	$\frac{16+\sqrt{6}}{360}$
$11-20$	$\left(hA_{+}\cos\left(\frac{2\pi k}{10}\right), hA_{+}\sin\left(\frac{2\pi k}{10}\right)\right)$	$\frac{16-\sqrt{6}}{360}$

Table 1: Points and weights a quadrature over a circle of order 10 where h is the radius of the circle, $k = 1, \ldots, 10$, and $A_{\pm} = \sqrt{\frac{6\pm\sqrt{6}}{10}}$

3 Optics

In order to describe the BES synthetic diagnostics, the code take in account:

- the beam geometry
- the energy components of the beam
- the sampling volume
- the finite lifetime effect
- the tokamak geometry
- the optical filters
- ADD OR REMOVE ITEMS

3.1 2D Numerical Integration

In order to compute the effect of the sightline, a 2D integration over a cirlce has to be done. To do so, a 2D quadrature formula is used with the weight and the points given in Table 1[1]. The order of this method is 10.

For computing the solid angle occupied by the lens from a point (P) in the sightline, an integration of $\Omega = \iint_S \frac{\hat{\mathbf{r}}\cdot\hat{n}}{r^2}\mathrm{d}S$, where S is the surface collecting the light, $\mathbf{r}$ is the vector from P to the surface, and $\hat{n}$ is the unit vector normal to the surface, has to be done. Three different case are possible: ADD DRAWING

- The ring has no importance,
- The lens has no importance,
- The two have to be taken in account.

For the first two cases, the integration can be done analytically and has been done in [8]. The result is given in (5) where L is the distance between the plane containing the disk, $R_{\max}$ (R_1) is the maximal (minimal) distance between the point and the disk, K is the complete integral of the first kind, $k^2 = 1 - \frac{R_1}{R_{\max}}$, Λ_0 is the Heuman's lambda function, $\xi = \arctan\frac{L}{|r_0 - r_m|}$, r_0 is the distance between P and the axis perpendicular to the disk and passing at its center, and r_m is the radius of the disk.

$$\Omega = \begin{cases} 2\pi - \frac{2L}{R_{\max}}K(k) - \pi\Lambda_0(\xi,k) & r_0 < r_m \\ \pi - \frac{2L}{R_{\max}}K(k) & r_0 = r_m \\ -\frac{2L}{R_{\max}}K(k) + \pi\Lambda_0(\xi,k) & r_0 > r_m \end{cases} \tag{5}$$

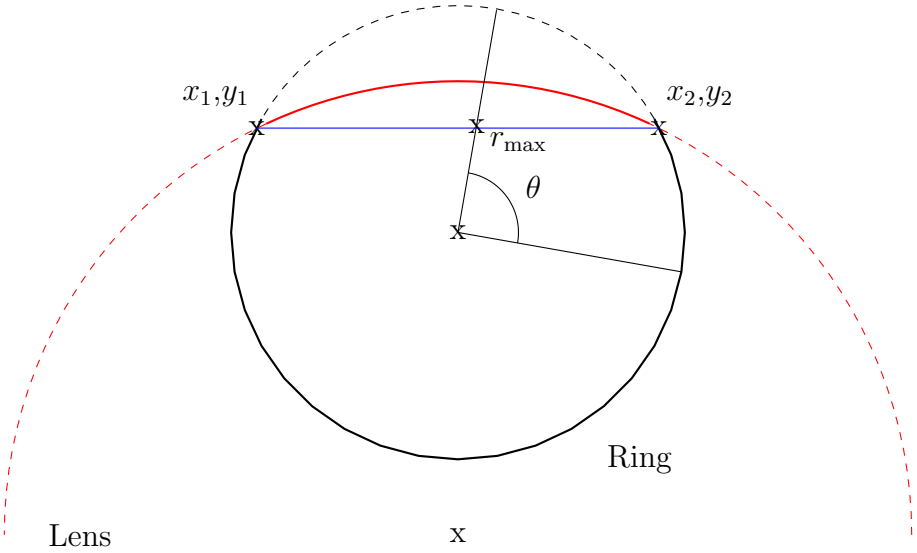

Figure 1: View from a point of the ring and the lens. The surface S receiving the photons is inside the black and red thick lines

3.2 Mixed case for the solid angle

For the last case, the integration is more complicated. Therefore a numerical integration has been done, and the formula is given in (6) where S is the surface of the object (see figure 1), S_i is a circle sector of the object, $r_{\max}$ is the maximal radius at the angle θ, ω are the weight for the radius and the angle, and $\Delta\theta$ is the angle covered by the circle sector.

$$\begin{aligned}\iint_S f(r,\theta)\mathrm{d}r\mathrm{d}\theta &= \sum_i \iint_{S_i} f(r,\theta)\mathrm{d}r\mathrm{d}\theta \\ &= \sum_i \int \frac{1}{2}\sum_j r_{\max}(\theta)\omega_{r,j} f(r_j,\theta)\mathrm{d}\theta \\ &= \frac{\Delta\theta}{4}\sum_{i,j,k} r_{\max}(\theta_k)\omega_{\theta,k}\omega_{r,j} f(r_j,\theta_k)\end{aligned} \tag{6}$$

L is the distance between the lens and the ring, z is the distance between the point **P** and the lens, **x**/**y** is the coordinates (2D) of the intersection points on the ring/lens. We have three equations (equation (7)), two for the border of the disks (lens and ring) and the last one for the fact that the three points are aligned.

$$\begin{cases} x_1^2 + x_2^2 &= r_r^2 \\ y_1^2 + y_2^2 &= r_l^2 \\ \frac{\mathbf{y}-\mathbf{P}}{z} &= \frac{\mathbf{y}-\mathbf{x}}{L} \end{cases} \tag{7}$$

First the last equation is used for having a linear relation between **x** and **y**.

$$\mathbf{y} = \left(\mathbf{P} - \frac{z}{L}\mathbf{x}\right) f \tag{8}$$

where $f = \frac{1}{1-\frac{z}{L}}$. In the second part, we use the last equation in the second equation of (7) for having a relation between x_1 and x_2:

$$x_1 = \frac{1}{2P_1}\left(\frac{L}{z}\left[\mathbf{P}^2 - \left\{\frac{r_l}{f}\right\}^2\right] + \frac{z}{L}r_r^2 - 2P_2x_2\right) = A + Bx_2 \tag{9}$$

The last step is to compute the value of x_2 with the help of the first equation of (7):

$$x_2 = \frac{-2BA \pm \sqrt{4B^2A^2 - 4\left(A^2 - r_r^2\right)\left(B^2+1\right)}}{2\left(B^2+1\right)} \tag{10}$$

In the case where the argument of the square root is smaller than zeros, it means that we do not have a mixed case and therefore only the ring limits the solid angle of the emission

4 XGC1 code

XGC1 is a full-f electrostatic gyrokinetic ion-electron particle code, it uses the particle-in-cell (PIC) method. The code is specially written for the edge plasmas. The key idea of the gyrokinetic equations is averaging the Larmor motion. By this method, the direction of the perpendicular motion is removed from the variables (6D $\rightarrow$ 5D) and the equations do not need to resolve the fast gyro-motion, therefore the time step can be increased. The key features of the Larmor motion are still present in the gyrokinetic equations.

The equations solved by the code are given in (11) - (13)[2] where $\dot{\mathbf{X}}$ is the time derivative of the gyro-center position of a particle and $v_\parallel$ is its velocity along the magnetic field, $\bar{\mathbf{E}}$ is the gyro-averaged electric field, $\hat{b} = \mathbf{B}/B$, $\mu = v_\perp^2/2B$ is the magnetic moment, and $D = 1 + (v_\parallel/B)\hat{b} \cdot (\nabla \wedge \hat{b})$, ρ_i is the ions gyroradius, λ_{Di} the ion Debye lengths, $\bar{n}_i$ is the gyro-center ion density (electrons have a smaller gyroradius, therefore $\hat{n}_e \approx n_e$). The two first equations describe the gyro-averaged motion of the particles and the last one is the gyrokinetic Poisson equation.

$$\dot{\mathbf{X}} = \frac{1}{D}\left[v_\parallel \hat{b} + \left(\frac{v_\parallel^2}{B}\right)\nabla B \wedge \hat{b} + \frac{\mathbf{B} \wedge (\mu \nabla B - \bar{\mathbf{E}})}{B^2}\right], \tag{11}$$

$$\dot{v_\parallel} = -\frac{1}{D}\left(\mathbf{B} + v_\parallel \nabla B \wedge \hat{b}\right) \cdot \left(\mu \nabla B - \bar{\mathbf{E}}\right), \tag{12}$$

$$-\nabla_\perp \frac{\rho_i^2}{\lambda_{Di}^2} \nabla_\perp \Phi = e\left(1 - \nabla_\perp \rho_i^2 \nabla_\perp\right)(\bar{n}_i - n_e) \tag{13}$$

A PIC code simulate some particles by using the field and not the two particles interactions, therefore a charge deposit has to be done. The steps of the simulation are the following[2]:

- Apply the charge deposit method
- Compute the electric potential with the gyrokinetic Poisson equation
- Calculate the eletric field
- Write the output
- Evolve the particles

4.1 Construction of the mesh

The mesh of XGC1 consists of a few poloidal planes (n_p) where an unstructured triangular mesh is constructed. In order to simplify the construction of the mesh, all the poloidal planes have the same mesh.

In equation (14), the field-line following poloidal variable is introduced where B_T is the toroidal component of the magnetic field, $\mathbf{B}_P = \nabla\phi \wedge \nabla\psi$ with $\psi = RA_\phi$, $\mathbf{A}$ is the magnetic potential vector, and ds is on the surface of constant ϕ and ψ[2].

$$\lambda := \int \frac{B_T}{RB_P} \mathrm{d}s \tag{14}$$

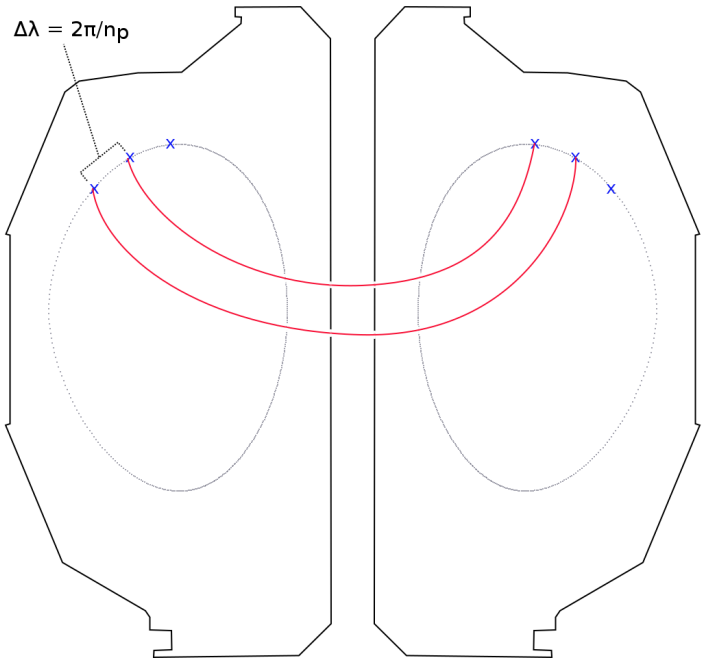

Figure 2: The grid (blue crosses) is constructed with the intersections between the poloidal plane and the field-line (red lines). The gray lines represent a magnetic flux surface. By this construction, the mesh respects the field-line following property.

The magnetic field can be written in the following way $\mathbf{B} = \nabla\psi \wedge \nabla(\lambda - \phi)$ and therefore $\lambda - \phi$ is constant along the B-field (and thus $\Delta\lambda = \Delta\phi = \frac{2\pi}{n_p}$). The integral needs a reference line and is computed using the method of characteristics and an ordinary differential equation solver. The mesh is constructed by using the intersection between the field lines and the poloidal plane (see figure **??**), therefore λ is used for the field-line following property (approximately applied). The point of the mesh are situated on a few magnetic flux surfaces (lines in a poloidal plane) and are separated by a distance of $\Delta\lambda = \frac{2\pi}{n_p}$.

Close to the X-point, the distance between two points becomes to small (due to the fact that $B_P \to 0$) and a minimal value for B_P (in the formula) is set: $\lambda := \int \frac{B_T}{R \max(B_P, B_{p0})} \mathrm{d}s$. An other problem comes from the part inside the separatrix, as the magnetic flux surfaces are closed, the requirement that $\Delta\lambda = \frac{\lambda_{2\pi}}{N}$ where $\lambda_{2\pi}$ is the variation in λ over one loop[2].

4.2 Output Files

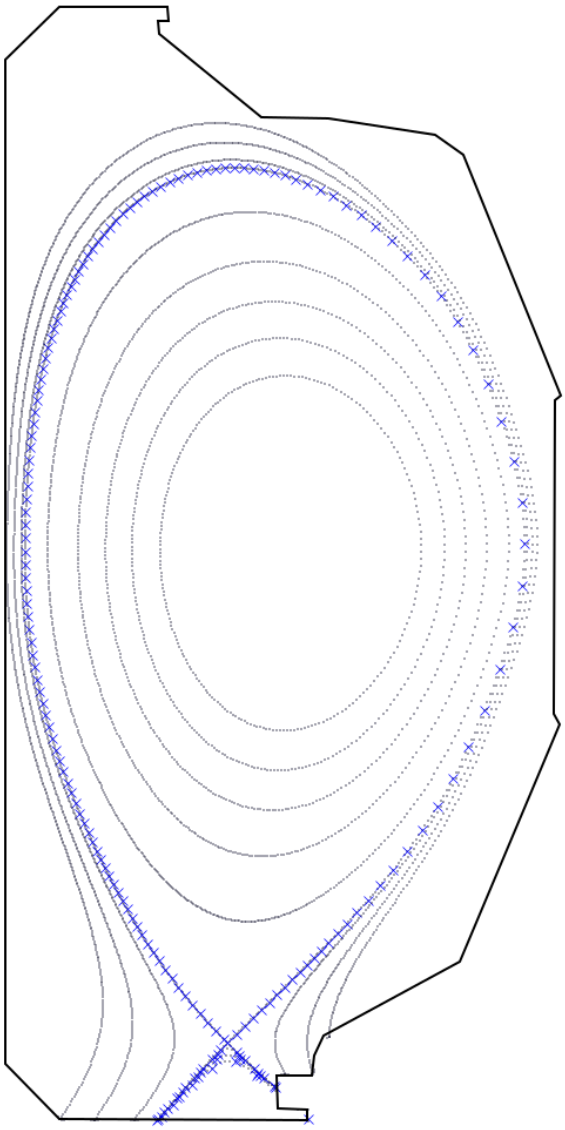

Figure 3: Example of mesh for the XGC1 code. The complete mesh is composed by n_p poloidal plane, and each one has the same mesh. The points of the mesh are situated on a few different magnetic flux surfaces (only a small sample is given in the figure), and the distance between two points of the same magnetic flux surface is given by λ (except inside the separatrix [approximately done] and around the X-point). The blue crosses are taken from a simulation, but only 20% of the points on this magnetic flux surface are shown

5 Annexes

5.1 Objectives at the beginning

- Understanding how the XGC1 code works
  - Understanding the general characteristics
  - Understanding the grid, the fluctuation in density and the data outputs
- Understanding the synthetic BES IDL code
  - Generalize the code for different reactors
  - Modify the IDL code for using the XGC1 outputs
  - (Optional) Translating the code in python
  - Extend to include further physics if needed
- Interpolation of $\tilde{n}_e$ along a field line
- Apply synthetic BES to previous XGC1 simulations and compare to experiment as possible
- (Optional) Compare specific DIII-D simulations with edge BES coverage

5.2 Description of the code

I tried to comment as much as possible the code, but I think it can be more easy if I explain the idea behind all the code in this report. For explaining the work, I follow the way that I created the code, I will start with the most basic classes and finish by the main class. A documentation has been done with sphinx in HTML[3].

ADAS

The first classes are the ADAS readers (that all inherite from an abstract class [`class ADAS_file`]). They are created for reading the ADAS database files and to simplify the acces to them. The code is reading only two kind of ADAS files, the 21 (`class ADAS21`) and the 22 (`class ADAS22`). The first one consists of the beam stopping coefficient and is used for computing the density of the beam, the second one is for the emission coefficient and is used when computing the emission of a specific place.

Collisions

The `class collisions` is used to interpolate the data from ADAS and computing a few quantities that depends on the collisions (for example the lifetime of the excited state or the wavelength of the emitted photons).

XGC1 Loader

The `class XGC1_Loader_BES` read the data from XGC1, store them, and, interpolate them with a field line interpolation.

Beam

The `class Beam1D` simulate the beam using the equilibrium data. It has the data from XGC1 as an attribute (under the shape of an instance of `XGC1_Loader_BES`). The emission is computed in this class too.

BES

The `class BES` uses `Beam1D` for computing the light received by the optical system. It is the highest level of the problem. It reads the data from a config file and use the method `get_bes()` to compute the diagnostics.

[3]if the link does not work, open the file ./html/FPSDP.html in your web browser

Bibliography

[1] M. Abramowitz and I. A. Stegun, editors. *Handbook of Mathematical Functions: with Formulas, Graphs, and Mathematical Tables*. Dover Publications, New York, 0009-revised edition edition, June 1965.

[2] M. F. Adams, S.-H. Ku, P. Worley, E. D'Azevedo, J. C. Cummings, and C.-S. Chang. Scaling to 150k cores: Recent algorithm and performance engineering developments enabling XGC1 to run at scale. *Journal of Physics: Conference Series*, 180(1):012036, July 2009.

[3] A. R. Field, D. Dunai, N. J. Conway, S. Zoletnik, and J. Sárközi. Beam emission spectroscopy for density turbulence measurements on the MAST spherical tokamak. *The Review of Scientific Instruments*, 80(7):073503, July 2009.

[4] C. Holland, A. E. White, G. R. McKee, M. W. Shafer, J. Candy, R. E. Waltz, L. Schmitz, and G. R. Tynan. Implementation and application of two synthetic diagnostics for validating simulations of core tokamak turbulence. *Physics of Plasmas (1994-present)*, 16(5):052301, May 2009.

[5] I. H. Hutchinson. Excited-state populations in neutral beam emission. *Plasma Physics and Controlled Fusion*, 44(1):71, Jan. 2002.

[6] K. Ikeda, M. Osakabe, A. Whiteford, K. Ida, D. Kato, S. Morita, K. Nagaoka, Y. Takeiri, K. Tsumori, M. Yokoyama, M. Yoshinuma, and L. Experiment. *J. Plasma Fusion Res. SERIES, Vol. 8 (2009) Optical Observation of Neutral Beam Attenuation in Hydrogen Discharge at LHD*. 2008.

[7] G. R. McKee, C. Fenzi, R. J. Fonck, and M. Jakubowski. Turbulence imaging and applications using beam emission spectroscopy on DIII-D (invited). *Review of Scientific Instruments*, 74(3):2014–2019, Mar. 2003.

[8] F. Paxton. Solid Angle Calculation for a Circular Disk. *Review of Scientific Instruments*, 30(4):254–258, Apr. 1959.

[9] M. W. Shafer, R. J. Fonck, G. R. McKee, C. Holland, A. E. White, and D. J. Schlossberg. 2d properties of core turbulence on DIII-D and comparison to gyrokinetic simulations. *Physics of Plasmas (1994-present)*, 19(3):032504, Mar. 2012.

[10] M. W. Shafer, R. J. Fonck, G. R. McKee, and D. J. Schlossberg. Spatial transfer function for the beam emission spectroscopy diagnostic on DIII-D. *Review of Scientific Instruments*, 77(10):10F110, Oct. 2006.